Appendix A: Derivation of porous electrode model

Following classic macroscopic porous electrode theory,[1] we first apply the differential form of the conservation of species i in the liquid phase of a control volume sized to include a representative volume of liquid and solid phases. We then integrate this conservation equation over the liquid volume, and use the divergence theorem and appropriate averaging to derive the following transport equation:

$$\psi \frac{\partial c_i}{\partial t} = -\overline{\nabla} \cdot \overline{N}_i + a j_{in} , \qquad [A1]$$

where ψ is the porosity of the porous medium, c_i is the concentration of species i volume averaged over the liquid phase of the control volume, N_i is the molar flux of species i averaged over total (solid and liquid) cross sectional area, j_{in} is the molar flux of i entering the liquid from the solid boundary averaged over the boundary area, and a is the surface area of boundary per unit volume of electrode. Assuming one-dimensional transport, dilute and binary electrolyte, electroneutrality, quiescent electrolyte, and no faradaic electrochemical reactions, we can write the following transport equations for the counter and co-ions in a porous, charging electrode:

$$\psi \frac{\partial c}{\partial t} = \psi F z_{count} v_{count} \frac{\partial}{\partial x}\left(c \frac{\partial \phi}{\partial x} \right) + \psi D_{count} \frac{\partial^2 c}{\partial x^2} + a j_{count} , \qquad [A2]$$

$$\psi \frac{\partial c}{\partial t} = \psi F z_{co} v_{co} \frac{\partial}{\partial x}\left(c \frac{\partial \phi}{\partial x} \right) + \psi D_{co} \frac{\partial^2 c}{\partial x^2} + a j_{co} . \qquad [A3]$$

Here z is the ion valence, v is the ion mobility (in units mol·s/kg), D is the ion diffusivity, and where the subscripts $count$ and co refer to the counter and co-ion respectively. Also, j_{count} and j_{co} are, respectively, the interfacial, area-averaged fluxes of counter- and co-ions entering the bulk liquid phase from the thin electric double layer (EDL) along the solid wall. If we further assume a symmetric electrolyte with equal mobilities, subtracting Eq. A3 from A2 (using $z_{co} = -z_{count}$), and replacing for the electromigration flux term in Eq. A2 yields the following transport equation:

$$\frac{\partial c}{\partial t} = D \frac{\partial^2 c}{\partial x^2} + \frac{a}{2\psi}(j_{count} + j_{co}) . \qquad [A4]$$

We now couple our model to the transient charging of a simple Helmholtz-type EDL. A Helmholtz EDL is modeled as two parallel layers of oppositely signed charge, where charges reside in fixed planes (similar to a conventional parallel plate capacitor).[2,3] Since the liquid side of the EDL contains no co-ions, $j_{co} = 0$. Also, a Helmholtz EDL has a linear (voltage independent) capacitance, and so for step potential charging, $j_{count} = -(C_{DL}/z_{count}F)\partial\phi/\partial t$, where C_{DL} is the EDL capacitance per unit area, F is Faraday's constant, and ϕ is the potential of the bulk liquid. Thus, our conservation of species equation in a porous electrode coupled to a charging Helmholtz EDL is:

$$\frac{\partial c}{\partial t} = D\frac{\partial^2 c}{\partial x^2} - \frac{C}{2\psi F z_{count}}\frac{\partial \phi}{\partial t}.$$ [A5]

Where C is the electrode capacitance per unit electrode volume ($C = C_{DL}{\cdot}a$). Equation A5 has both concentration and potential as unknowns. To develop a second equation, we first define the superficial liquid-phase current density, i_l, as:

$$i_l = F\sum_i z_i N_i.$$ [A6]

Next, we write the conservation of bulk liquid phase current in our two-phase control volume as:

$$\frac{\partial i_l}{\partial x} = aF z_{count} j_{count} = -C\frac{\partial \phi}{\partial t}.$$ [A7]

Summing Equation A6 over our binary, symmetric electrolyte with equal anion and cation diffusivities, we can derive a form of Ohm's law:

$$i_l = -\psi\sigma\frac{\partial \phi}{\partial x}.$$ [A8]

Where σ is the local conductivity of the liquid phase, and $\sigma = 2F^2 z_{count}^2 vc$. Combining Equations A7 and A8 yields the governing equation for potential:

$$\frac{\partial \phi}{\partial t} = \frac{\psi}{C}\frac{\partial}{\partial x}\left(\sigma\frac{\partial \phi}{\partial x}\right).$$ [A9]

Derivation of cell RC time constant

To derive an expression for the resistance of our cell, we first describe the ionic resistance of a porous medium. We assume a pore structure of n non-intersecting, uniform cross sectional area, tortuous capillaries. The resistance of the porous medium is therefore that of n capillaries in parallel:

$$R = \frac{L_p}{n\sigma A_p}.$$ [A10]

Here, L_p is the length of the tortuous pore, and A_p its cross section area. We now introduce the porosity as the ratio of void volume to total volume of the porous medium, $\psi = nA_p L_p/(AL)$, where A is the cross sectional area of the porous medium and L its length (in the electric field direction):

$$R = \frac{L}{\sigma\psi A}\frac{L_p^2}{L^2} = \frac{LT}{\sigma\psi A}.$$ [A11]

Here, $T = (L_p/L)^2$ is the tortuosity of the pore structure. We can then formulate the resistance of our cell as that of two electrodes and a separator in series, where we assume the electrodes and separator have equal porosities and tortuosities:

$$R_{cell} = \frac{(2l_e + l_s)T}{\psi \sigma A}.$$

[A12]

Lastly, the capacitance of our cell is half the capacitance of an electrode, and so $2C_{cell} = CAl_e$. Note that in our derivation, we did not explicitly account for the effect of a bimodal pore size distribution on electrode resistance (*i.e.*: the effect of the etched nanoscale porosity). We hope to address such refinements of the model as part of future work.

Appendix B: Additional information on measurements

Measurements of extracted desalted stream concentration

In Figure 6, we showed concentration reductions for twelve experimental conditions ($c_o = 50$, 100, and 250 mM, $V = 0.75$, 1, 1.25, and 1.5 V). The data at $c_o = 100$ mM was shown in Figure 5. We here show the data for $c_o = 50$ and 250 mM.
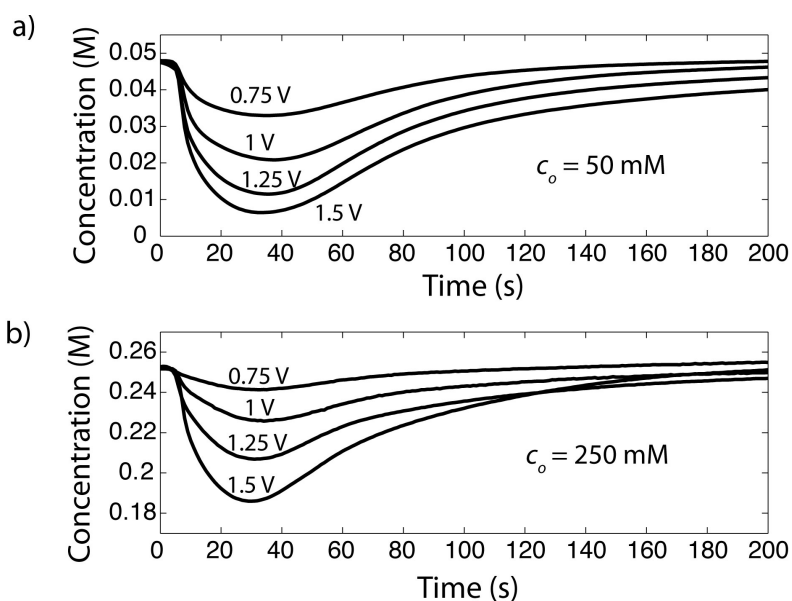

Figure B1: Concentration of the extracted stream from the charged cell *vs.* time for initial concentrations of a) 50 mM, and b) 250 mM. In all cases, the minimum concentration of the extracted stream decreases with increasing potential. At $c_o = 50$ mM, relatively little additional concentration reduction is achieved at 1.5 V compared to 1.25 V, consistent with the plateau-like trend observed in Figure 6 of the text.

Capacitance measurements

We performed the following to measure capacitance of our cell: We filled the cell with the NaCl solution of interest, as described in the Experimental Methods section. With flow stopped, we then charged the cell by applying a step potential and measured the current response. After some time (typically 10-45 min) current approximately reached steady state (that is, the current value decreased by roughly 1% per minute or less). At this steady state, the value of current was assumed to be equal to the cell's leakage current. We then flowed new solution through the cell at 0.5 mL/min while maintaining the applied potential. We noticed a repeatable, sudden increase in measured current as new solution began to flow through the cell (Fig B2 inset). We continued to hold the potential and maintain flow until current reached a steady state again. To estimate cell capacitance, C_{cell}, we subtracted the leakage current from the measured current response, integrated this result, and divided the integral by applied voltage. To calculate electrode volume specific capacitance, we multiplied the cell volume specific capacitance by a factor of 4 (we assumed symmetric electrodes). We also measured the discharge current upon application of zero volts across the electrodes, and integrating this curve gave us approximately the same result for capacitance.

Figure B2 shows the results of the measured cell capacitance at twelve experimental conditions. We measured a maximum electrode capacitance of about 8.4 F at 250 mM, 1.5 V, which corresponds to an electrode specific capacitance of about 130 F/g of dry electrode weight or 40 F/cc of electrode volume. Figure B2 inset shows two current response *vs.* time curves for the conditions of 100 mM, 1 V (solid line), and 100 mM, 1.5 V (dotted line). As the data shows, current rises suddenly upon onset of the flow, increasing by over 1 mA for 1 V applied, and over 5 mA at 1.5 V.

We included the flow step in the aforementioned protocol in order to measure the equilibrium capacitance of the cell when the pore bulk concentration is that of the initial NaCl solution. During the charging process, salinity is decreased in the electrode's pores bulk, which can cause a significant decrease in pore EDL capacitance due to the thickening of the EDL.[2] We attribute the sudden increase in current observed upon flowing new, undesalted solution through the charged pores to a sudden increase in EDL capacitance.
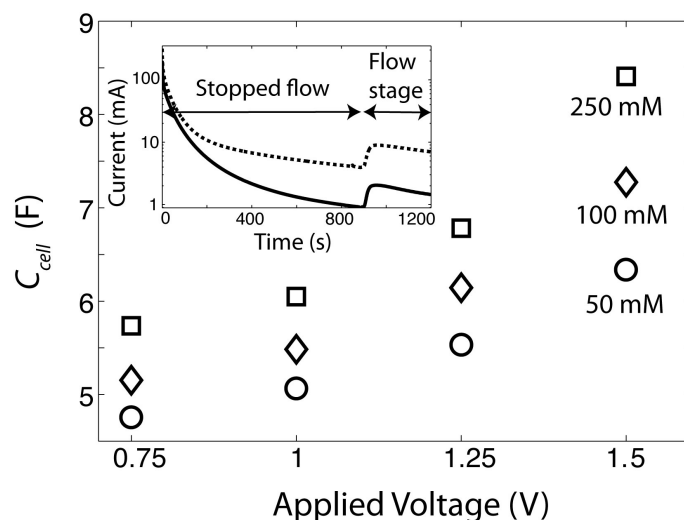
Figure B2: Measured capacitance of our FTE CD cell versus applied voltage, and for various initial NaCl salinities (250 mM: squares, 100 mM: diamonds, 50 mM: circles). Cell capacitance increases with NaCl concentration and applied voltage, reaching a maximum of about 8.4 F at 250 mM, 1.5 V. Inset shows two example current response curves obtained upon application of a step potential at $t = 0$ of 1 V (solid line) and 1.5 V (dotted line), with $c_o = 100$ mM. Cell charging proceeds until roughly 900 s, at which point we flow new 100 mM NaCl solution through the cell, and observe a rapid increase in current.

Charge efficiency measurements

In Figure B3, we show measurements of charge efficiency at our 12 experimental conditions. We obtained these by dividing the total salt removed from the bulk solution by the total electric charge stored. Total salt removed was obtained by integrating the concentration *vs.* time figures (Fig. 5 and B1) and multiplying by flow rate (0.5 mL/min). Total electric charge was obtained by integrating under the current *vs.* time curves, including both the stopped flow (charging) stage and the flow stage (see Fig B2 inset). The charge efficiency increased with increasing applied potential between 0.75 and 1.25 V and decreasing ionic strength. Between 1.25 V and 1.5 V, charge efficiency plateaued or slightly decreased, which may be due to the effects of the higher measured leakage current at these higher voltages. The maximum charge efficiency measured was about 0.43 at 50 mM and 1.25 V.
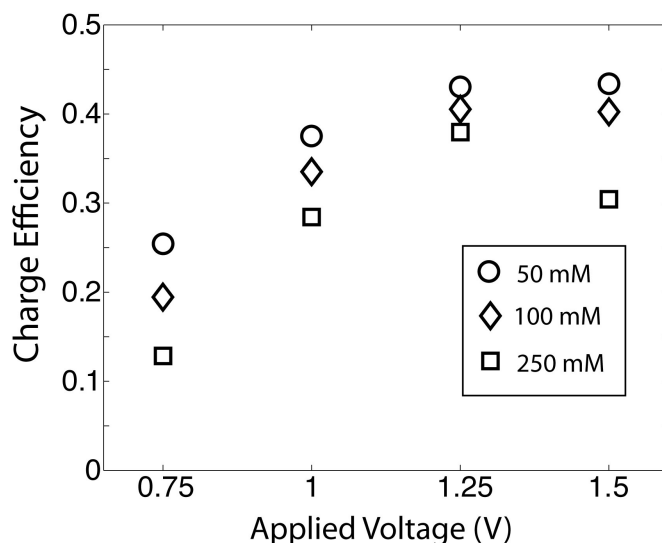
Figure B3: Measurements of charge efficiency *vs.* applied voltage for various sodium chloride concentrations. Charge efficiency increased with potential from 0.75 to 1.25 V, and then plateaued or slightly decreased from 1.25 to 1.5 V. Charge efficiency increased with decreasing concentration.

Tortuosity measurements

We obtained estimates of electrode tortuosity, T_e, through measurements of pressure required to flow through our FTE CD cell. For these measurements, we used our cell with the Millipore separator (with 5 µm diameter pores), so that the hydraulic resistance of the separator was negligible relative to that of the HCAM electrodes. We measured a pressure of 3.9 kPa at 0.5 mL/min flow rate, and pressure varied approximately linearly with flow rate. We then calculated T_e using a known relation for flow rate and pressure drop across a porous media:[4]

$$T_e = \frac{\psi_e A a^2}{8 \mu L} \frac{\Delta p}{Q} .$$
[B1]

Here, a is the micron-scale pore radius, which is about 0.6 µm for our HCAM electrodes (see Figure 3), μ is solution viscosity, L is the length of the porous substrate (2 mm for back to back HCAM electrodes), and A is the substrate cross sectional area. Using a flow rate of 0.5 mL/min, and the measured pressure of 3.9 kPa, we obtained $T_e = 3.6$.

Series resistance measurements

We estimate that R_s was roughly one order of magnitude higher than an estimate of our separator resistance, $R_{sep} = (l_s T_s)/(\psi_s A \sigma_o)$. We calculated R_{sep} using known separator geometry and porosity, and assuming a separator tortuosity, T_s, of unity. We attribute this result to a possible higher than unity tortuosity of the separator pore structure and to the possible presence of a gap between elements in our cell (a contact resistance). The separator is 25 µm thick, and so a relatively small gap of 100 µm could

give rise to a significant contact resistance, highlighting the importance of separator dimensions and the cell assembly process.

REFERENCES

1. J. Newman and K. E. Thomas-Alyea, *Electrochemical Systems*, John Wlley & Sons, Inc., Hoboken, NJ, 2004.
2. R. J. Hunter, *Zeta Potential in Colloidal Science, Principles and Applications*, Academic Press, New York, 1981.
3. L. L. Zhang and X. S. Zhao, *Chem. Soc. Rev.*, 2009, **38**.
4. S. H. Yao and J. G. Santiago, *J. Colloid Interface Sci.*, 2003, **268**, 133-142.